Experimental Study of Smooth Asymmetric Compound Channels Flow: An Investigation of the Interaction of Flow Using Scaling Argument for Prediction of Overall Discharge

P Singh[1], X Tang[*], Y Guan[3]

Department of Civil Engineering, Xi'an Jiaotong-Liverpool University, Suzhou, 215123, China
Email: Xiao.Tang@xjtlu.edu.cn

Abstract. A simple model for the apparent shear stress on the vertical interface between the floodplain and main channel in asymmetric smooth compound channels is proposed using experimental data obtained in this study. The turbulent structure, including Reynolds shear stress in asymmetric compound channel flows, is investigated for three different flow depths. The lateral distribution of the apparent shear stress obtained shows that the total apparent shear stress has a negative peak near the junction edge in the main channel. Furthermore, the intensity of the advection terms and the Reynold shear stress near the interface are investigated as the function of the bankfull height and floodplain width. The momentum transport due to Reynolds stress and secondary current between main channel and floodplain is finally modeled as depth ratio using scaling argument. The validation of the current model on three datasets shows an accurate prediction of overall discharge for the asymmetric smooth compound channels.
Keywords: Overall discharge, asymmetric compound channel, Momentum transfer, turbulent shear, secondary current

1. Introduction

The decrease in velocity in the different sections of compound channels, intensifies as the depth somewhat reaches just above the bankfull height [1-3]. Thereafter, the decrease in channel velocity would directly relate to the retarding effect of apparent shear force. For the modelling purpose, a good approximation of the apparent shear stress on the interface is needed to accurately predict the discharge over the flooded areas. Accuracy of the predicted apparent shear (τ_a) at the interface of the compound section occurring on the interfacial vertical, horizontal or diagonal plane helps to improve 1D methods, which are lucid to apply and can be corrected to predict overall discharge and zonal discharge [4-9]. Apparent shear can be defined as a measure of the combining effect of viscous shear, turbulence with the action of vortices induced between main-channel and floodplain(s) [3, 10]. Two components of large-scale motions, namely the fluctuation velocity ($\overline{\tau_{yx}}$) and secondary current ($\rho\overline{uv}$) where ρ is the fluid density and $\overline{uv}$ is the time average product of streamwise and lateral velocity, are key characteristics to measure momentum exchange in any compound channel [11-15]. However, in practice, measuring τ_a is time consuming and cumbersome because small scale (in time and size) vortices are difficult to capture. Therefore, researchers generally relate τ_a to large-scale motions, such as mean velocity. The overall τ_a is often approximated as a function of the difference between main channel (U_c) and floodplain (U_f) velocity [16-19].

The aforementioned approach is identified in the linear scaling argument by describing the lateral momentum transfer between adjacent flow sections [20]. This lateral momentum transfer is usually introduced as the interfacial stress (τ_{int}) between the corresponding sections. Our contention lies on the same hypothetical assumption where in the streamwise direction, the largest eddy scale is observed as the typical difference in average velocity due to no-slip condition at the channel bed. This paper aims to investigate the characteristics of spanwise shear stress due to the advection induced secondary currents, Reynolds shear stress, and then the apparent shear stress, which represents the magnitude of the spanwise momentum transport. Finally, a scaling argument model for interfacial shear stress is proposed to estimate the overall discharge of an asymmetric compound channel.

2. Experimental Methodology

The experiments were carried out in a 0.75m wide and 20m long glassed-wall flume at the hydraulics laboratory of Xi'an Jiaotong Liverpool University (XJTLU), China (figure 1). Three compound channel cross sections were tested in the rectangular flume with the bed slope of S_0 =0.003 in all the scenarios. The three test asymmetrical channels has the bankfull height of 4 and 8 cm with the floodplain width of 20 and 40cm, respectively (figure 1b). In total, three depth ratios for each configuration are tested and designated as low depth (D_r=0.1), intermediate depth (D_r=0.3) and high depth (D_r=0.5). In the experiments, the main channel Manning's roughness n is found to be 0.01. The floodplain material is polyvinyl chloride (PVC), used to construct three different cases of the experiments (table 1). In table 1, Q_t is the total flow discharge of channel; U_{mc} and U_{fp} are the main channel and floodplain velocity respectively; Reynolds number $Re = U_{ave}R/\vartheta$, where R is the hydraulic radius and ϑ is kinematic viscosity; and Froude number $Fr = U_{ave}/\sqrt{g(H-h)}$, where g is the acceleration due to gravity.

The flow depths were measured using point gauges, while discharges were measured by an electromagnetic flowmeter installed in front of the channel at the upstream end. The 3D velocities were measured using side and down looking Acoustic Doppler velocimeter (ADV) at the cross section located at the 10m downstream from the entrance. For all the tests, uniform flow condition remains with the averaging flow depth being discrepancies of ± 4 mm between 5 and 18 m sections. The x-, y- and z-axes refer to streamwise, transverse and vertical (normal to the bed) directions, respectively. The corresponding instantons velocities, time averaged velocities and velocity fluctuations are denoted as (u,v,w), (U, V, W) and (u', v', w'), respectively. The measuring points in a cross-section were taken at an interval of 5 mm vertically and at the interval of 20 to 50 mm laterally. Also, measurements were obtained by averaging time series at 50Hz over 60-120 mins. The accuracy of the ADV was ± 1 to 3% of the measured mean velocities and ± 7 to 10% for the Reynolds stresses. The ADV raw data were processed with the software WinADV using the [21] filtering method based on de-spiking concept.

Table 1. Summary of the flow conditions of all test cases where test names signify first three numbers as floodplain width and last digit as bankfull height.

Tests	Dr (=1-h/H)	Q_t (l/s)	U_{ave} (m/s)	U_{mc} (m/s)	U_{fp} (m/s)	Re ($\times 10^4$)	Fr	$\overline{-u'_x u'_y}/U_{x,int}{}^2$
R0204	0.1	16.83	0.3786	0.4146	0.0978	4.90	0.5605	0.1083
	0.3	21.14	0.4315	0.4564	0.1390	7.16	0.5755	0.0464
	0.5	35.23	0.5161	0.5208	0.2509	12.4	0.5821	0.0118
R0208	0.1	40.27	0.3294	0.3054	0.1735	13.2	0.5402	0.0145
	0.3	40.43	0.4926	0.4864	0.1707	14.4	0.4683	0.0121
	0.5	40.50	0.5076	0.5537	0.1334	13.8	0.2637	0.0120
R0404	0.1	16.81	0.3296	0.5173	0.2003	2.77	0.4999	0.1795
	0.3	21.14	0.4034	0.5892	0.2645	5.82	0.5179	0.1133
	0.5	25.32	0.4669	0.6571	0.4368	9.36	0.5306	0.0101

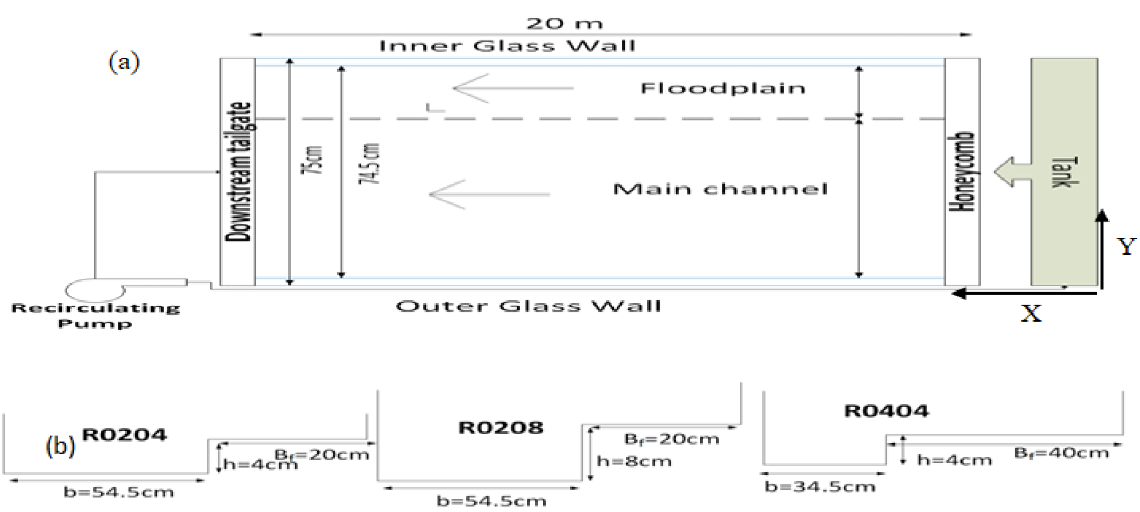

Figure 1. (a) Plan view and (b) cross-sections of the three asymmetric compound channels.

3. Cross-sectional Variation of Flow Variables

3.1. The Lateral Distribution of the Depth-Averaged Streamwise Velocity

Figure 2 shows the depth-averaged streamwise velocity for nine test cases in table 1. To obtain the depth-averaged values for hydrodynamic parameters, these cross-sectional measurements are averaged over depth and time, which is usually called double average. For normalization, the double-averaged value of the interfacial velocity ($U_{x,int}$) is used in practice, as shown in [22]. On the contrary, other parameters like friction velocity (U_*) or the velocity scale defined as the difference of main-channel (U_{mc}) and floodplain (U_{fp}) divided by the characteristic length at the interface [23-25]. In our study, the foremost priority should be given to the significant effect of the channel geometry and the flow depth on the interfacial region velocity, so the depth-averaged interface velocity plays a key role in understanding the behavior of flow. Furthermore, the flow type in a compound channel is classified as shallow flow when $D_r < 0.3$, and intermediate flow when $0.3 < D_r < 0.5$ [26-27]. The characteristics of the shallow flow are established as the monotonic and large gradient of velocity flow at the interface, as shown in figure 2. A significant difference can be observed over the interfacial region for $D_r \leq 0.3$ against $D_r > 0.3$ where the lateral variation of velocity is small. The 2D macro-vortices over the horizontal plane near the interface ($y/B_f = 1$) are induced due to the sudden change of geometry from main-channel to floodplain. The floodplain width in R0404 is twice that of R0204, and the velocity distribution in the two different geometries is strongly dependent on the momentum exchange over the interface. Moreover, the lateral variation of $U_{x,d}$ over the interfacial region in the case of a wider floodplain (R0404) is smaller than the cases like R0204 and R0208, indicating the strong effect of width ratio on the momentum transfer of flow between main-channel and floodplain.

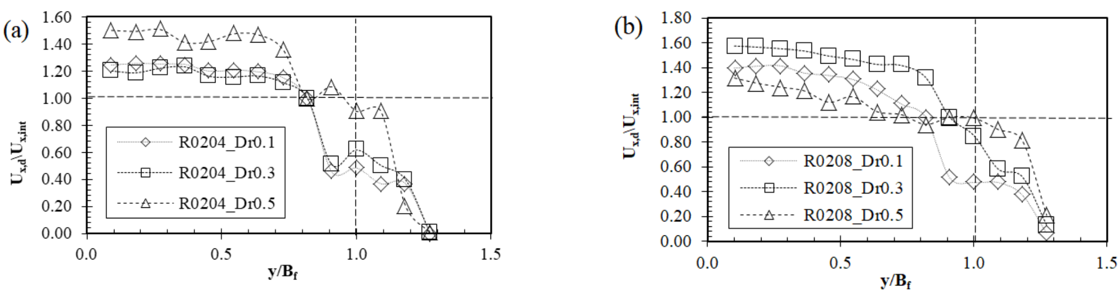

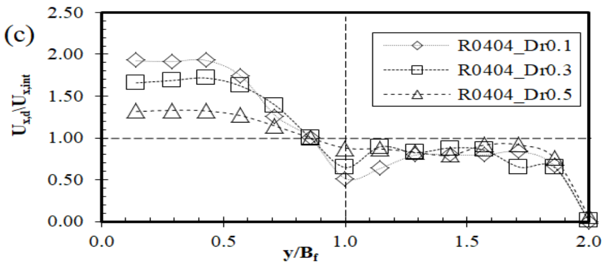

Figure 2. Distribution of normalized depth-averaged velocity over the cross section for (a) R0204; (b) R0208; (c) R0404. The standard errors estimated for all three cases are 1%, 3% and 1%, respectively.

3.2. Depth-Averaged Reynolds Stress

Figure 3 shows the lateral distribution of the normalized Reynolds stress ($\overline{-u'_x u'_y}/U_{x,int}{}^2$) for different flow depths under shallow flow ($D_r < 0.3$) and intermediate flow ($0.3 < D_r < 0.5$) regime for three configurations. The Reynolds shear stress is generally related to the gradient of the streamwise mean velocity. Figure 3 clearly shows that the maximum value of the Reynolds shear stress occurs at the interface where $y/B_f = 1$. Shiono and Knight [28] also experimentally observed that the highest value of Reynolds shear is generally seen near the free surface in the interfacial shear zone. In all our tests, the most notable fluctuation of Reynolds shear stress is in the shallow flow region, with the maximum at $D_r = 0.1$. On the contrary, the lateral variation of $\overline{-u'_x u'_y}$ for the flow condition of $D_r = 0.5$ is found to be very small over the interface. Even for the channel having a higher bankfull height (R0208), there is a visible change in the lateral gradient of velocity over the two sections (figure 3b). The peak at the interface (i.e., $y/B_f = 1$) is significant for the case of $D_r < 0.3$, although it is not valid for the case of $D_r = 0.5$ where a higher flow exists in the floodplain. Moreover, the effect is not as noteworthy compared to other cases like figure 3 (a, c). Table 1 also shows the normalized peak values of $\overline{-u'_x u'_y}/U_{x,int}{}^2$ at the interface ($y/B_f = 1$) for all nine tests.

The peak value for $\overline{-u'_x u'_y}/U_{x,int}{}^2$ is found to shoot at $y/B_f = 1$ for shallow depths, as also pointed by [24]. Interestingly, the peak of Reynolds stress is somewhat smaller in the case of R0208, which points to the reduced turbulent kinetic energy. Indicatively, the water depth in the main channel for this case is comparatively high, so the mixing length does not grow proportionally to the shear layer generation over the interface. In other words, in these conditions, the wall induced turbulence overpowers the shear layer based turbulence. Furthermore, turbulence in deeper bankfull height is no more dominant by the bottom turbulence, especially in the main channel section. Usually on contrary, for shallow depth conditions, the lateral velocity gradients are undermined over bottom turbulence experienced over the interface; however, it is otherwise in R0208.

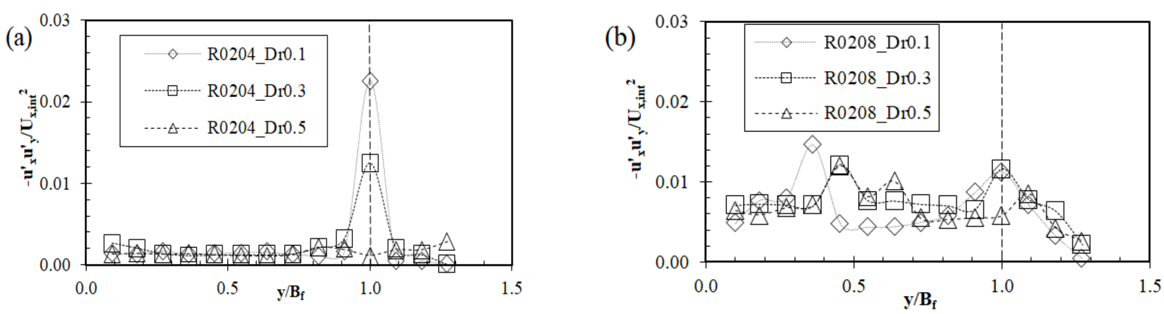

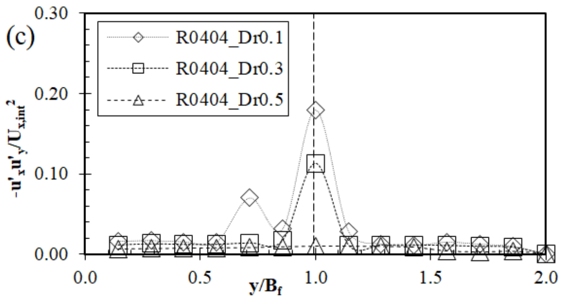

Figure 3. Lateral distribution of the dimensionless transverse Reynolds stress for (a) R0204; (b) R0208; and (c) R0404. The standard error for this parameter was about 7-10% in overall cases with a maximum of 9.8% in R0208.

4. Flow Interaction and Effects of Transverse Currents on Main Channel and Floodplain

For the fully developed flow in the section with steady uniform flow, the momutem equation can be deduced to [8]:

$$(H-h)\left(\rho\overline{uv}-\overline{\tau_{yx}}\right)= \rho g A S_o - \tau_b P \quad (1)$$

where A and P are the area and wetted perimeter of the main-channel, respectively. By rearranging Eq. (1), the apparent shear stress τ_a $(=\rho\overline{uv}-\overline{\tau_{yx}})$ becomes $\tau_a = \frac{(\rho g A S_o - \tau_b P)}{H-h}$.

In figure 4 (a-c), the magnitude of spanwise momentum transport is depicted through apparent shear stress in the transverse direction of the cross section. The experimental data in figure 4 show the apparent shear stress attains a negative peak near the interface of the main channel and floodplain, irrespective of the higher depth ratio (D_r=0.5). [23, 29-30] indicated that the apparent shear stress became extremely large as the depth ratio decreases, which is depicted in all the experimental results illustrated in figure 4. They have also identified that the Reynolds stress term is expected to be dominant compared to the advection term. Therefore, it is essential to estimate the magnitude of momentum transport due to Reynolds stress and secondary currents between the main channel and the floodplain in asymmetric compound channel flow, as a function of floodplain width and depth ratio.

4.1. Interface Stresses on Linear Scale Argument

Van Prooijen et al. [12] and Bousmar and Zech [31] have derived interfacial stresses for compound channels, demonstrating the lateral momentum transfer in shallow mixing layers using scaling arguments. In general, the apparent shear stress τ_a $(=\rho\overline{uv}-\overline{\tau_{yx}})$ has two components: advection due to secondary currents, and shear stress due to the Reynolds stress. By assuming the largest eddy scale as a typical difference of streamwise velocities, i.e. the order of the mean flow in each compartment of compound channel, the interfacial velocity is estimated as an average of the main channel (U_c) and floodplain (U_f) velocity [18]. The a can be expressed as $\tau_a = \frac{1}{2}\varphi\rho({U_c}^2 - {U_f}^2)$.

The dimensionless interface coefficient φ is estimated from the experiments done in this study in the transverse direction for all the cases (see table 2).

Table 2. Dimensionless coefficient φ for parameters h/b_f and Dr for asymmetrical compound channels.

Test case / Depth ratio (Dr)	R0204	R0208	R0404
	h/b_f = 0.2	h/b_f = 0.4	h/b_f = 0.1
0.1	0.0331	0.0654	0.0305
0.3	0.0251	0.0127	0.0204
0.5	0.0150	0.005	0.0160

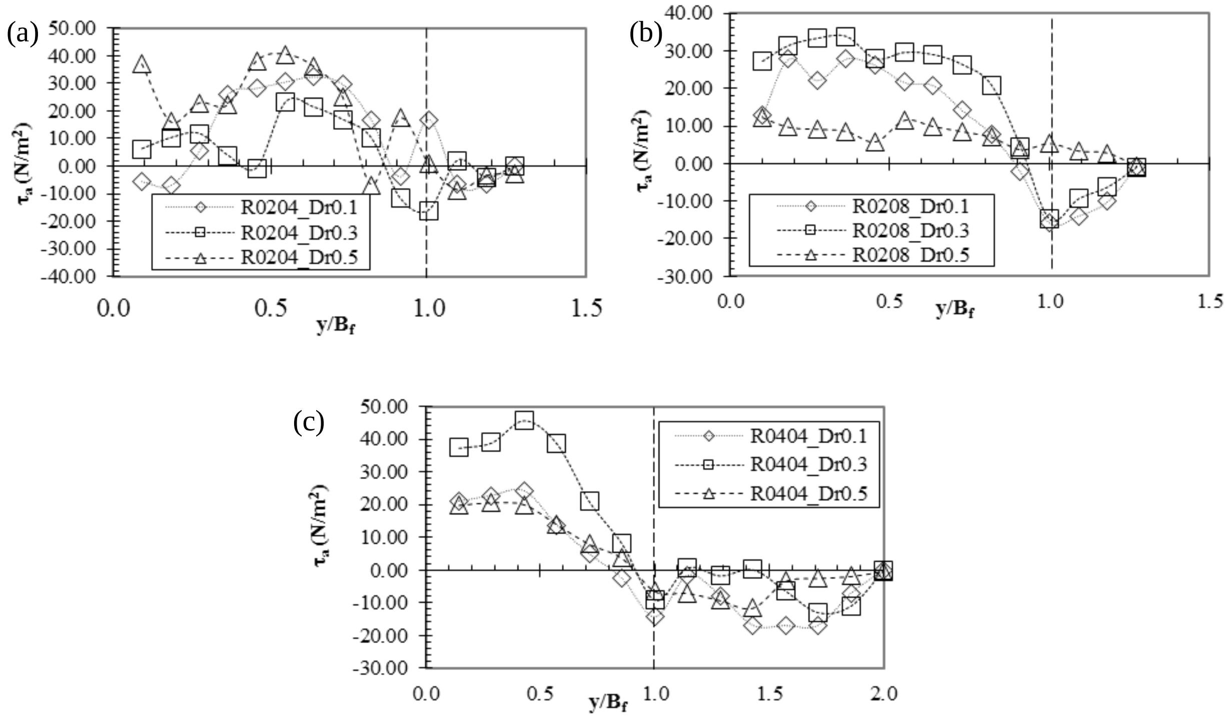

Figure 4. Spanwise distribution of apparent shear stress τa for (a) R0204, (b) R0208 and (c) R0404.

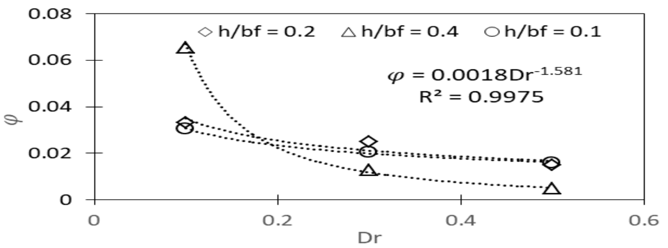

Figure 5. Correlation of the vertical interface coefficient φ of apparent shear friction to the depth ratio Dr for the range of $0.1 \leq \mathrm{h/b_f} \leq 0.4$ in our experiments.

Figure 5 shows the vertical interface coefficient φ of apparent shear friction against depth ratio D_r for three h/b_f data. The data points suggest a power function to estimate interfacial stress at the vertical junction with the coefficient of determination as R^2= 0.99. Based on the above argument, a very simple function as $\varphi = 0.0018Dr^{-1.581}$ is found to hold true for the data range of $0.1 \leq h/b_f \leq 0.4$ with smooth asymmetric compound channels.

5. Validation of the Current Model for Discharge Calculations

The classical divided channel method (DCM) and vertical divisional line DCM (QDCMV) are commonly used for discharge estimation, which is based on the Manning's Eq. (2). Much commercial software like HEC based modules, CES (Wallingford), and others use the DCM in their algorithms. In spite of simplicity, the DCM overshoots the overall discharge estimation because it does not take momentum transfer into account [32-33].

$$Q = \frac{1}{n} A R^{\frac{2}{3}} S_o^{\frac{1}{2}} \quad \text{or} \quad Q = \left[\sum_{i=1}^{n} \left(\frac{1}{n_i} A_i R_i^{\frac{2}{3}}\right)\right] S_o^{\frac{1}{2}} \tag{2}$$

where n is the Manning's coefficient, R is the hydraulic radius, i.e. the ratio of the wetted area (A) to perimeter (P), and i denotes the subsection as main channel c or floodplain f.

To overcome the problem of overestimation in DCM-based methods, the effect of apparent shear stress at the vertical interface between the subsections of an asymmetric channel is included in the model as a weighting factor. Thus, a coefficient ω_i is included in the QDCM (V) methods as:

$$\omega_m = 1 - \frac{\tau_a P_a}{\rho g A_m S_o} \text{ and } \omega_f = 1 + \frac{A_m}{A_f}(1 - \varphi_m) \tag{3}$$

$$Q_{m=}Q'_m \omega_m^{0.5} \text{ and } Q_{f=}Q'_f \omega_f^{0.5} \tag{4}$$

where the weightage of the boundary shear force to the fluid flow for each section is defined as ω_m, ω_f; $P_a = 2(H - h)$ is the perimeter on which effective apparent shear force acts. The actual main channel and floodplain discharges are defined as Q_m, Q_f, while Q'_m, Q'_f are the discharges estimated through classical QDCM (V) without considering the effect of momentum transfer at the interface.

Table 3. Experimental and river datasets used in the analysis.

Data	Q_t (m^3/s)	h/Bf	b/B	b/b_f	b_f/B	L/B	D_r=(H-h)/H
[34]	0.0140-0.0373	0.12	0.4942	0.9772	0.5058	22.35	0.1843-0.5434
[35]	0.2235-0.9292	0.06	0.3846	0.6667	0.5769	15.39	0.0522-0.5031
[36]	0.0035-0.0058	0.25	0.2000	0.2500	0.8000	20.00	0.1844-0.2607

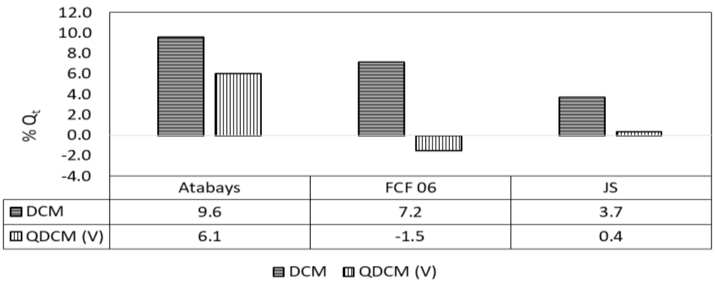

Figure 6. Prediction of total discharge % Q_t using DCM and QDCM (V) with Eq. 4, which is the present modeled equation for the coefficient of apparent shear friction on the vertical interface φ.

Twenty-eight homogenously smooth data of asymmetric experimental channels are considered in the validation of the present model (see table 3). The range of data varies from $0.0522 \le Q_t \le 0.5434$ in m^3/s, $0.00103 \le S_o \le 0.0103$, $0.0013 \le Dr \le 0.8182$.

The error percentage between predicted and experimental total discharge for each flow depth is calculated as $\%Q_t = \frac{|Q_{cal.i} - Q_{exp,i}|}{Q_{exp,i}} \times 100\%$, where $\%Q_t$ is the relative error percentage of the predicted and observed discharge at i_{th} flow depth, respectively. Figure 6 shows the percentage of errors of the predicted discharge for all the datasets.

6. Conclusions

The experimental results for the spanwise apparent shear stress obtained in the asymmetric compound channel are used here to propose a new model for predicting the overall discharge, which is based on the lateral momentum transfer parameter using the scaling argument. The model is easy to use and has only one parameter defined as the coefficient φ of apparent shear friction on the vertical interface. This dimensionless coefficient φ is found to have a power function with the depth ratio for the geometrical range of $0.1 \leq h/b_f \leq 0.4$ for the asymmetric smooth compound channels. The application of the new model gives a good agreement for the datasets in comparison to the DCM that overestimates the results in every case. However, the results obtained in our model are well within the reasonable percentage error with a maximum of 6.1% in our test datasets. The overall conclusion shows that the present experimentally calibrated model for interfacial stress has potential and can be extended to the rough asymmetric compound channels.

Acknowledgments
The grant for this study was funded by National Natural Science Foundation of China (No. 11772270), the Research Fund (Key Special Fund (KSF-E-17, RDF-16-02-02) of XJTLU.

References
[1] Sellin R H J 1964 A laboratory investigation into the interaction between the flow in the channel of a river and that over its flood plain *La Houille Blanche* (7): 793-802.
[2] Zheleznyakov G V 1971 Interaction of channel and flood plain *Proceeding of the 14th Congress of the IAHR* **5**: 144-148.
[3] Myers W R C 1978 Momentum transfer in a compound channel *Journal of Hydraulic Research* **16**(2): 139-150.
[4] Tang X 2018 Evaluating methods for discharge prediction of straight asymmetric compound channels *Journal of Geological Resource and Engineering* **6**(5).
[5] Tang X 2018 A method for improving stage discharge prediction in asymmetric compound channels *Proceedings of 2018 International Conference on Environmental and Water Resources Engineering* (pp. 63-70).
[6] Tang X 2019 Lateral Shear Layer and Its Velocity Distribution of Flow in Rectangular Open Channels *Journal of Applied Mathematics and Physics* **7**(04): 829-840.
[7] Tang X 2019 A new apparent shear stress-based approach for predicting discharge in uniformly roughened straight compound channels *Flow Measurement and Instrumentation* **65**: 280-287.
[8] Singh P, Tang X & Rahimi H R 2020 Modelling of the apparent shear stress for predicting zonal discharge in rough and smooth asymmetric compound open channels *River Flow 2020 Proceedings of the 10th Conference on Fluvial Hydraulics* (Delft, Netherlands 7-10 July 2020) (p. 84). CRC Press.
[9] Singh P & Tang X 2020 Zonal and overall discharge prediction using momentum exchange in smooth and rough asymmetric compound channel flows *Journal of Irrigation and Drainage Engineering* **146**(9): 05020003.
[10] Singh P K & Tang X 2020 Estimation of apparent shear stress of asymmetric compound channels using neuro-fuzzy inference system *Journal of Hydro-Environment Research* **29:** 96-108.
[11] Singh P, Tang X, & Rahimi H R 2019 Apparent shear stress and its coefficient in asymmetric compound channels using gene expression and neural network *Journal of Hydrologic Engineering* **24**(12): 04019051.
[12] Van Prooijen B C, Battjes J A & Uijttewaal W S 2005 Momentum exchange in straight uniform compound channel flow *Journal of hydraulic engineering* **131**(3): 175-183.
[13] Proust S, Riviere N, Bousmar D, Paquier A, Zech Y & Morel R 2006 Flow in compound channel with abrupt floodplain contraction *Journal of Hydraulic Engineering* 132(9) 958-970.
[14] Tang X & Knight D W 2009 Analytical models for velocity distributions in open channel flows *Journal of Hydraulic Research* **47**(4): 418-428.
[15] Chen Z, Chen Q & Jiang L 2016 Determination of apparent shear stress and its application in compound channels *Procedia Engineering* **154**: 459-466.

[16] Wormleaton P R & Merrett D J 1990 An improved method of calculation for steady uniform flow in prismatic main channel/flood plain sections *Journal of Hydraulic Research* **28**(2): 157-174.
[17] Christodoulou G C 1992 Apparent shear stress in smooth compound channels *Water Resources Management* **6**(3): 235-247.
[18] Huthoff F, Roos P C, Augustijn D C & Hulscher S J 2008 Interacting divided channel method for compound channel flow *Journal of Hydraulic Engineering* **134**(8): 1158-1165.
[19] Moreta P J & Martin-Vide J P 2010 Apparent friction coefficient in straight compound channels *Journal of Hydraulic Research* **48**(2): 169-177.
[20] Wormleaton P R, Allen J & Hadjipano P 1982 Discharge assessment in compound channel flow *Journal of the Hydraulics Division* **108**(9): 975-994.
[21] Goring D G, & Nikora V I 2002 Despiking acoustic Doppler velocimeter data *Journal of Hydraulic Engineering* **128**(1): 117-126.
[22] Proust S & Nikora V I 2020 Compound open-channel flows: effects of transverse currents on the flow structure *Journal of Fluid Mechanics* 885.
[23] Tominaga A & Nezu I 1991 Turbulent structure in compound open-channel flows *Journal of Hydraulic Engineering* **117**(1): 21-41.
[24] Uijttewaal W S J & Booij R 2000 Effects of shallowness on the development of free-surface mixing layers *Physics of Fluids* **12**(2): 392-402.
[25] Dupuis V, Proust S, Berni C & Paquier A 2017 Mixing layer development in compound channel flows with submerged and emergent rigid vegetation over the floodplains *Experiments in Fluids* **58**(4): 30.
[26] Stocchino A & Brocchini M 2010 Horizontal mixing of quasi-uniform straight compound channel flows *Journal of Fluid Mechanics* **643**: 425.
[27] Nezu I 1999 Coherent horizontal vortices in compound open-channel flows *Hydraulic Modeling*.
[28] Shiono K & Knight, D W 1991 Turbulent open-channel flows with variable depth across the channel *Journal of Fluid Mechanics* **222**: 617-646.
[29] Rajaratnam N & Ahmadi R 1981 Hydraulics of channels with flood-plains *Journal of Hydraulic Research* **19**(1): 43-60.
[30] Singh P K, Tang X, & Rahimi H 2020 A Computational Study of Interaction of Main Channel and Floodplain: Open Channel Flows *Journal of Applied Mathematics and Physics* ***8***(11): 2526-2539.
[31] Bousmar D & Zech Y 1999 Momentum transfer for practical flow computation in compound channels *Journal of Hydraulic Engineering* **125**(7): 696-706.
[32] Knight D W & Demetriou J D 1983 Flood plain and main channel flow interaction *Journal of Hydraulic Engineering* **109**(8): 1073-1092.
[33] Prinos P & Townsend R D 1984 Comparison of methods for predicting discharge in compound open channels *Advances in Water Resources* **7**(4): 180-187.
[34] Atabay S 2001 *Stage-Discharge, Resistance and Sediment Transport Relationships for Flow in Straight Compound Channels* University of Birmingham.
[35] University of Birmingham 2001 *Flow Database* [online] Accessed June 15, 2019 *http://www.flowdata.bham.ac.uk*.
[36] Joo C B H & Seng D M Y 2008 Study of flow in a non-symmetrical compound channel with rough flood plain *J. Inst. Eng.* **69** (2): 18–26.